Copy
RM E54L02

C.2

Unavailable
UNCLASSIFIED

NACA RM E54L02

CLASSIFICATION CHANGED
UNCLASSIFIED
By authority of TPA #29 Date 8-19-46
Unavailable

RESEARCH MEMORANDUM

FLIGHT INVESTIGATION OF PENTABORANE FUEL IN 9.75-INCH-DIAMETER RAM-JET ENGINE AT LOW EQUIVALENCE RATIO

By Merle L. Jones and John H. Disher

Lewis Flight Propulsion Laboratory
Cleveland, Ohio

CLASSIFIED DOCUMENT

This material contains information affecting the National Defense of the United States within the meaning of the espionage laws, Title 18, U.S.C., Secs. 793 and 794, the transmission or revelation of which in any manner to an unauthorized person is prohibited by law.

NATIONAL ADVISORY COMMITTEE
FOR AERONAUTICS

WASHINGTON

March 29, 1957

Unavailable

NATIONAL ADVISORY COMMITTEE FOR AERONAUTICS

RESEARCH MEMORANDUM

FLIGHT INVESTIGATION OF PENTABORANE FUEL IN 9.75-INCH-DIAMETER RAM-JET ENGINE AT LOW EQUIVALENCE RATIO

By Merle L. Jones and John H. Disher

SUMMARY

In order to investigate the performance of pentaborane fuel at relatively low equivalence ratios, a second flight was made with a 9.75-inch-diameter ram-jet engine using pentaborane at an average equivalence ratio of approximately 0.23. The engine was launched from a carrier airplane at a pressure altitude of 32,000 feet and a free-stream Mach number of 0.57. It accelerated to a free-stream Mach number of 1.74 in 37 seconds, with a peak acceleration of 1.65 g's being reached in 33 seconds. A flame-out, which is believed to have been a result of oxide deposits plugging the fuel spray bar, occurred at approximately 37 seconds. An average combustion efficiency of 94 percent was obtained under severe combustor-inlet conditions of high velocities and low pressures and temperatures. The pentaborane was observed to give approximately a 96 percent increase in relative range over that previously observed for JP-3 fuel in flight under similar conditions.

A maximum thrust coefficient of 0.392 was reached at a free-stream Mach number of 1.44, a maximum propulsive thrust coefficient of 0.242 was reached at a free-stream Mach number of 1.00, and a maximum drag coefficient of 0.191 was reached at a free-stream Mach number of 1.32.

INTRODUCTION

The initial flight investigation of the performance of pentaborane fuel in a 9.75-inch-diameter ram-jet engine at comparatively rich fuel-air ratios (equivalence ratio ≈ 0.55) is reported in reference 1. The pentaborane was observed to have a relative range approximately 70 percent greater than hydrocarbon fuel operating under similar flight conditions. The improvement was the result of a higher heating value and higher combustion efficiencies. At equivalence ratios appreciably lower than 0.55, even greater improvements in relative range are indicated by theory and by test-stand investigations. In order to substantiate these indications by means of actual flight tests, a second flight was made

with a 9.75-inch-diameter ram-jet engine using pentaborane at an average equivalence ratio of approximately 0.23. The ram jet was launched from an F-82 carrier airplane at a pressure altitude of 32,000 feet and a free-stream Mach number of 0.57. The performance data obtained from the flight are presented herein.

SYMBOLS

The following symbols are used in this report:

A_{max}	maximum cross-sectional area, 0.534 sq ft
a_n	axial acceleration (exclusive of gravity component), g's
C_D	drag coefficient, D/q_0A_{max}
C_F	thrust coefficient, F/q_0A_{max}
C_F-C_D	propulsive thrust coefficient, $\frac{a_nW_e}{q_0A_{max}}$
D	drag, lb
F	thrust, lb
f/a	fuel-air ratio
M	Mach number
m	mass flow, slugs/sec
m_0	mass flow in free-stream tube equal in area to cowl-lip capture area, slugs/sec
P	total pressure, lb/sq ft abs
p	static pressure, lb/sq ft abs
q	dynamic pressure, 0.7 pM^2, lb/sq ft
R	gas constant
Re	Reynolds number based on body length of 9.87 ft

S_a air specific impulse, lb-sec/lb air

T total temperature, $^{\circ}R$

t static temperature, $^{\circ}R$

V velocity, ft/sec

W_e engine weight at any given instant, lb

w_f fuel flow, lb/hr

η_b combustion efficiency, $\left(\frac{\varphi_{theor}}{\varphi_{exp}}\right)_{S_a=constant} \times 100$

μ ratio of gas flow at engine exit to engine air flow

τ total-temperature ratio, T_6/T_0

φ equivalence ratio; ratio of actual to stoichiometric fuel-air ratio

Subscripts:

0 station at free stream

1 station at inlet

2 station in diffuser $21\frac{1}{4}$ inches downstream of inlet

3 station at diffuser exit $65\frac{1}{4}$ inches downstream of inlet

4 fictitious station which has the same total pressure and air flow as station 3 but has an area equal to that at station 5

5 station immediately downstream of flame holder

6 station at exit

B behind a normal shock

APPARATUS AND INSTRUMENTATION

A photograph of the ram-jet engine mounted on the carrier airplane is shown in figure 1. A sketch of the engine, which has a design free-stream Mach number of 1.8, is shown in figure 2. The engine was the same as that described in reference 1 with the following exceptions:

(1) The length of the ignition flare in the center of the flame holder was extended from 3 to 8 inches so that the burning time was increased from 20 to 45 seconds. A photograph of the modified flame holder is shown in figure 3.

(2) The fuel-tank material was changed from Inconel to aluminum, resulting in a decrease in the gross weight of the engine from 156 to 143 pounds.

(3) The fuel spray-bar hub was reinforced to reduce the possibility of its burning off.

(4) The fuel control schedule was altered to give the desired lower fuel flow throughout the flight.

The instrumentation consisted of an eight-channel telemetering unit which transmitted the following information to two ground receiving stations:

(1) Free-stream static pressure, p_0

(2) Total pressure measured at the Pitot-static tube, P_0 or $P_{0,B}$

(3) Total pressure measured at the Pitot-static tube minus total pressure in the diffuser at station 2 ($21\frac{1}{4}$ in. downstream of inlet), $P_{0,B} - P_2$

(4) Total pressure measured at the Pitot-static tube minus diffuser-exit total pressure at station 3 ($65\frac{1}{4}$ in. downstream of inlet), $P_{0,B} - P_3$

(5) Total minus static pressure at station 2, $P_2 - p_2$

(6) Exit static pressure, p_6

(7) Fuel pressure at the spray-bar inlet minus diffuser-exit total pressure, $P_f - P_3$

(8) Axial acceleration (exclusive of gravity component), a_n

[redacted]

CALCULATION PROCEDURE

Calculations were made in a manner similar to that described in reference 1 with the following exceptions:

1. The total-pressure drop across the flame holder was assumed to be equal to 1.2 instead of 2 times the dynamic pressure upstream of the flame holder ($P_4 - P_5 = 1.2\ q_4$). The revised value was determined from cold-flow ground tests of the flame holder installed in the engine. Calculations indicate that, in the free-stream Mach number range observed in the flight reported in reference 1, the error in the values of thrust coefficient is slight when a flame-holder pressure drop of $2q_4$ is assumed.

2. The more rigorous calculation procedure presented in reference 2 was used to account for the effects of the nongaseous exhaust products on exit flow conditions and for the variation in the combustor-outlet static pressure.

RESULTS AND DISCUSSION

The time histories of the flight conditions encountered by the ram jet are presented in figure 4. Included in the figure are curves of axial acceleration (exclusive of gravity component), free-stream Mach number, free-stream total and static pressures, free-stream total and static temperatures, and Reynolds number. The Reynolds number is based on a body length of 9.87 feet. After release from the airplane at a pressure altitude of 32,000 feet and a free-stream Mach number of 0.57, the ram jet accelerated to a free-stream Mach number of 1.74 in 37 seconds at which time the engine began to decelerate. At 37.2 seconds, the transmission of the telemeter data terminated because of transmitter failure. The pressure altitude of the engine at this time was 5100 feet. A peak acceleration of 1.65 g's was reached at 33 seconds. At 37 seconds, it appears that combustion ceased with a resulting deceleration.

The time histories of the combustion-chamber conditions are presented in figure 5. The combustion-chamber inlet static pressure increased from 1/3 to nearly $2\frac{1}{2}$ atmospheres while the calculated inlet static temperature increased from 430° R to 765° R during the flight. The calculated total-temperature ratio τ across the combustion chamber (fig. 5(b)) was approximately constant between 11 and 22 seconds, decreased gradually until approximately 32 seconds, and then fell off rapidly. The decreasing acceleration and the rapidly decreasing total temperature ratio, both of which began at approximately 32 seconds, are believed to have been caused by plugging of the spray bar by solid oxide

deposits from the burning fuel. Figure 5(c), which is a time history of the actual and the scheduled fuel pressure, shows that the fuel pressure continued to rise throughout the flight in accordance with the fuel control schedule. Since the scheduled fuel flow provided for a minimum τ of about 3.5 based on a 90-percent combustion efficiency, the falling heat release after 32 seconds must have been caused by either a rapidly falling combustion efficiency or a change in the fuel-spray-bar pressure-flow relation. It is believed that the latter explanation is the more logical one. As a result, test-stand runs are being made on a revised fuel-spray-bar - flame-holder configuration which is designed to be less susceptible to the forming of solid deposits over the spray-bar holes.

In addition to the total-temperature ratio, figure 5(b) presents curves of combustion efficiency η_b and fuel-air ratio f/a. During the period from 11 seconds to 30 seconds, the average combustion efficiency was 94 percent. The falling efficiency after 22 seconds may indicate the start of fuel-spray-bar plugging. However, the plugging, if present, was slight until 30 seconds. Thereafter, the fuel-air-ratio and combustion-efficiency data are considered unreliable and are not presented.

Fuel flow w_f, combustion-chamber inlet velocity V_4, and combustion-chamber inlet Mach number M_4 are presented in figure 5(d). During the interval from 11 seconds to 30 seconds, when the average combustion efficiency was 94 percent, the combustion-chamber inlet velocity ranged from 150 to 300 feet per second. These velocities, together with the low pressures and temperatures which were encountered, provide a severe combustion test of the fuel. Maximum efficiencies of the order of 70 percent were observed for gasoline-fueled engines in flight under similar conditions (ref. 3).

Figure 6 presents the combustion efficiency against equivalence ratio φ with indicated values of combustor-inlet static pressure expressed in atmospheres. Also shown on the figure are efficiencies observed during connected-pipe tests of pentaborane (ref. 2) and the values obtained in flight at higher equivalence ratios (ref. 1). The values of η_b greater than 1.0 are indicative of the limit of the experimental accuracy.

Figure 7 shows the variation of mass-flow ratio m/m_0 with free-stream Mach number M_0. Also shown is the theoretical maximum mass-flow ratio, which for this inlet equals 1.0 near the design free-stream Mach number of 1.8. The change in slope of the observed mass-flow-ratio curve at an M_0 of about 1.45 coincides with the decreasing acceleration and total-temperature ratio at approximately 32 seconds. At an M_0 of approximately 1.62, m/m_0 reached the theoretical maximum value of 0.960,

indicating critical flow at that point. No data are shown beyond this point, because the air-flow differential pressure measurement at station 2 went beyond the range of the instrumentation. However, supercritical flow existed for the remainder of the flight so that mass-flow ratios equal to the theoretical value would be expected.

Pressure Recovery

The total-pressure recoveries at station 2 P_2/P_0 and at the diffuser exit P_3/P_0 are shown as a function of free-stream Mach number in figure 8. The diffuser buzz which was encountered in the initial flight at $M_0 > 1.23$ was eliminated in this flight as a result of a leaner fuel-air mixture and higher mass-flow ratios. The total-pressure recovery at the inlet improved correspondingly in the supersonic Mach number range. Curves of P_2/P_0 and P_3/P_0 from the initial flight (ref. 1) are included in figure 8 for purposes of comparison. The observed recovery at station 2 for the flight being reported herein was approximately equal to the theoretical value up to an M_0 of about 1.6, after which supercritical flow existed. The total-pressure recovery in the diffuser between stations 2 and 3 varied from 95 to 91 percent up to an M_0 of 1.4. The appreciably higher subsonic flow losses of the second flight, as compared with the first flight, are caused by the higher mass-flow ratios and the higher diffuser velocities. At the higher Mach numbers, the total-pressure loss between the two stations increased rapidly. The rapidly increasing pressure loss was caused by increasing friction losses as the mass-flow ratio and diffuser velocity increased and by internal shock losses when supercritical flow was encountered.

Thrust, Propulsive Thrust, and Drag Coefficients

The thrust coefficient C_F is presented in figure 9 as a function of M_0. Also shown in the figure are indicated values of the total temperature ratio parameter $\mu^2 \frac{R_6}{R_5} \frac{T_6}{T_0}$. The thrust coefficient increased rapidly with increasing Mach number up to a Mach number of approximately 1.1 when the total-temperature-ratio parameter began to decrease. In the Mach number range from 1.1 to 1.5, the effect of the decreasing total-temperature-ratio parameter was counteracted by the effect of the increasing Mach number, so that the thrust coefficient remained nearly constant during that period. The decreasing thrust coefficient after an M_0 of 1.5 corresponds to the rapidly falling total-temperature ratio and diffuser total-pressure recovery. A maximum thrust coefficient of

0.392 was reached at a free-stream Mach number of 1.44. No data points are presented at Mach numbers lower than 0.90 because of a questionable accuracy in the calculations for the exit Mach number for this particular flight. No data points are presented at Mach numbers over 1.62 because of the lack of air-flow data. At Mach numbers greater than 1.33 (after 30 sec), extrapolated values of fuel flow were used in the calculations for C_F.

The propulsive thrust coefficient $C_F - C_D$ is presented with indicated values of $\mu^2 \frac{R_6}{R_5} \frac{T_6}{T_0}$ in figure 10 as a function of M_0. The thrust-minus-drag force is obtained directly from acceleration measurements, so that the previously described limitations in calculating thrust coefficient at the beginning and end of the flight do not apply here. A maximum value of 0.242 was reached at a free-stream Mach number of 1.00. The drop and subsequent rise in the propulsive thrust coefficient between Mach numbers of 1.0 and 1.4 is caused by the rise and subsequent drop in the drag (see fig. 11) during the same period. The decreasing propulsive thrust coefficient after an M_0 of 1.45 corresponds to the decreasing thrust coefficient shown on figure 9.

The curve of drag coefficient against M_0 is shown on figure 11. The drag coefficient reached a maximum value of 0.191 at a free-stream Mach number of 1.32. Because of the higher mass-flow ratios for this flight, the drag was appreciably lower than for the flight discussed in reference 1.

Comparison with Hydrocarbon Fuel

A graph comparing the performance of pentaborane and JP-3, in terms of relative range, is shown in figure 12. For the purpose of this report, relative range is defined as the ratio of the range of a vehicle with a given fuel and combustion efficiency to the range of a similar vehicle operating under the same flight conditions with JP-3 fuel and 100-percent combustion efficiency. In accordance with reference 4, the relative range was assumed to be directly proportional to the fuel weight specific impulse, the effect of fuel density being slight for the two fuels considered here. Figure 12 gives the relative ranges for pentaborane and JP-3 with 100-percent combustion efficiency and also with actual combustion efficiencies observed under flight conditions. The fuel weight specific impulse values for both fuels operating with 100 percent combustion efficiency were calculated from data presented in reference 5. The relative range of the pentaborane, under actual flight conditions, is based on the observed combustion efficiencies, while that of the JP-3 fuel is based on the combustion efficiency obtained with

JP-3 fuel in the 16-inch-diameter engines which are reported in reference 3. The two values presented in figure 12 for pentaborane are the average of the values which were calculated for the period of the flight from 15 to 30 seconds during which time the average equivalence ratio was 0.23. With pentaborane, the average ideal (100-percent combustion efficiency) relative range for this period during the flight was 1.43, while the actual average relative range was 1.37 - a difference of 4 percent. The average actual relative range of the JP-3 fuel, operating under similar flight conditions, was 0.70. Thus, at the lean equivalence ratio conditions of this flight, pentaborane has been observed to give approximately a 96-percent increase in relative range over that which was previously observed for JP-3 in flight under similar conditions. The corresponding increase observed during the initial flight, which operated at an average equivalence ratio of approximately 0.55, was approximately 70 percent. This improvement is a result of the combined effects of a higher heating value per pound of fuel and higher combustion efficiencies. If the same combustion efficiency were to be obtained with both fuels, the range improvement of pentaborane during the second flight would be reduced to 43 percent. Although these values were obtained at relatively low Mach numbers, the comparisons are applicable to high Mach numbers at high altitudes where combustor-inlet conditions are of a severity comparable to those encountered in this flight.

SUMMARY OF RESULTS

The second flight test of pentaborane fuel in a 9.75-inch-diameter air-launched ram-jet engine with a design free-stream Mach number of 1.8 has provided the following results:

1. The engine accelerated from a free-stream Mach number of 0.57 to a free-stream Mach number of 1.74 in 37 seconds, with a peak acceleration of 1.65 g's being reached in 33 seconds. A flame-out, which is believed to have been a result of oxide deposits plugging the fuel spray bar, occurred at approximately 37 seconds.

2. The average combustion efficiency during the period from 11 to 30 seconds was 94 percent. The high efficiencies were obtained under severe combustor conditions of high velocities and low pressures and temperatures.

3. Diffuser buzz or pulsing, which was encountered in the first flight at $M_0 > 1.23$, was eliminated in this flight as a result of operation at lower equivalence ratios and higher mass-flow ratios. The diffuser pressure recovery at the inlet improved correspondingly, being approximately equal to theoretical values up to a Mach number of 1.6, after which supercritical flow existed in the diffuser.

4. A maximum thrust coefficient of 0.392 was reached at a free-stream Mach number of 1.44, a maximum propulsive thrust coefficient of 0.242 was reached at a free-stream Mach number of 1.00, and a maximum drag coefficient of 0.191 was reached at a free-stream Mach number of 1.32.

5. The average relative range of pentaborane with respect to JP-3 at 100-percent combustion efficiency was 1.37 during the period of the flight from 15 to 30 seconds when the average equivalence ratio equaled 0.23. The pentaborane was observed to give approximately a 96-percent increase in relative range over that which was previously observed for JP-3 fuel in flight under similar conditions. If the same combustion efficiencies were to be obtained with both fuels, the range improvement of pentaborane would be reduced to 43 percent.

Lewis Flight Propulsion Laboratory
National Advisory Committee for Aeronautics
Cleveland, Ohio, December 6, 1954

REFERENCES

1. Disher, John H., and Rabb, Leonard: Initial Performance Investigation of Pentaborane Fuel in Free-Flight Ram-Jet Engine. NACA RM E54D28, 1957.

2. Fivel, Herschel J., Tower, Leonard K., and Gibbs, James B.: Pentaborane Combustion Performance in 9.75-Inch-Diameter Ram-Jet Engine in Connected-Pipe Altitude Facility. NACA RM E54I16, 1957.

3. North, Warren J.: Summary of Free-Flight Performance of a Series of Ram-Jet Engines at Mach Numbers from 0.80 to 2.20. NACA RM E53K17, 1954.

4. Henneberry, Hugh M.: Effect of Fuel Density and Heating Value on Ram-Jet Airplane Range. NACA RM E51L21, 1952.

5. Tower, Leonard K., and Gammon, Benson E.: Analytical Evaluation of Effect of Equivalence Ratio, Inlet-Air Temperature, and Combustion Pressure on Performance of Several Possible Ram-Jet Fuels. NACA RM E53G14, 1953.

Figure 1. - 9.75-Inch-diameter ram-jet engine mounted on carrier aircraft.

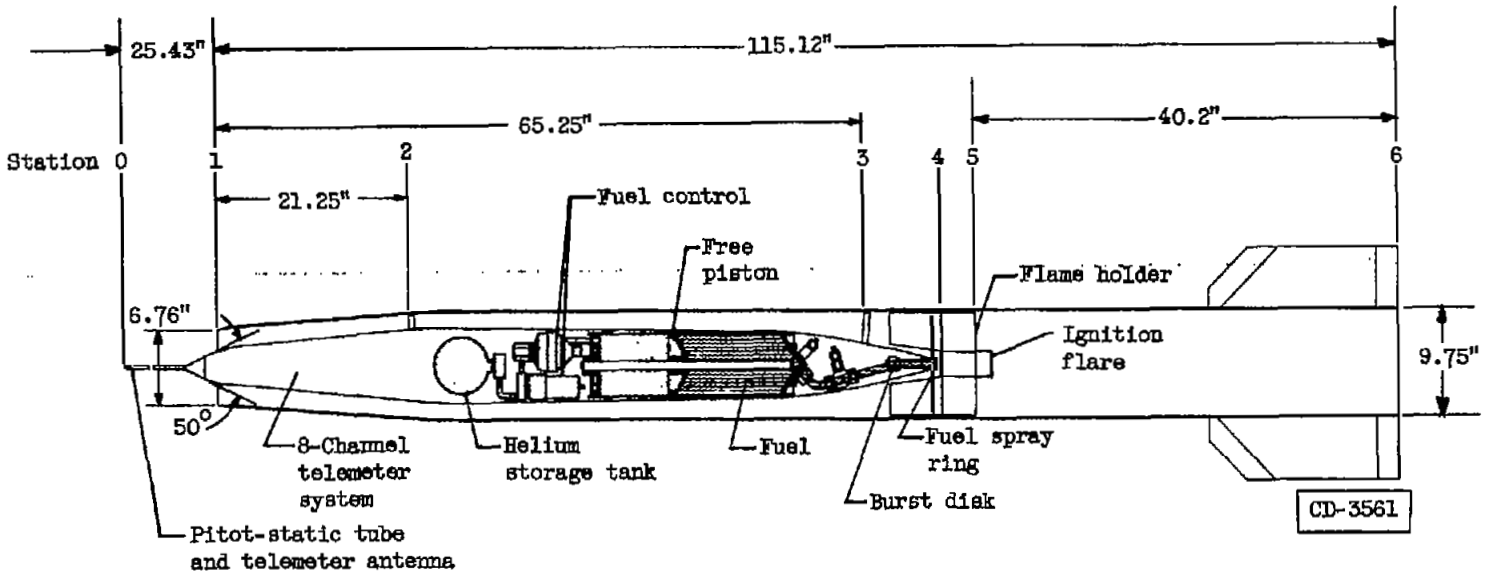

Figure 2. - Sketch of 9.75-inch-diameter free-flight ram-jet engine used in high-energy-fuel tests.

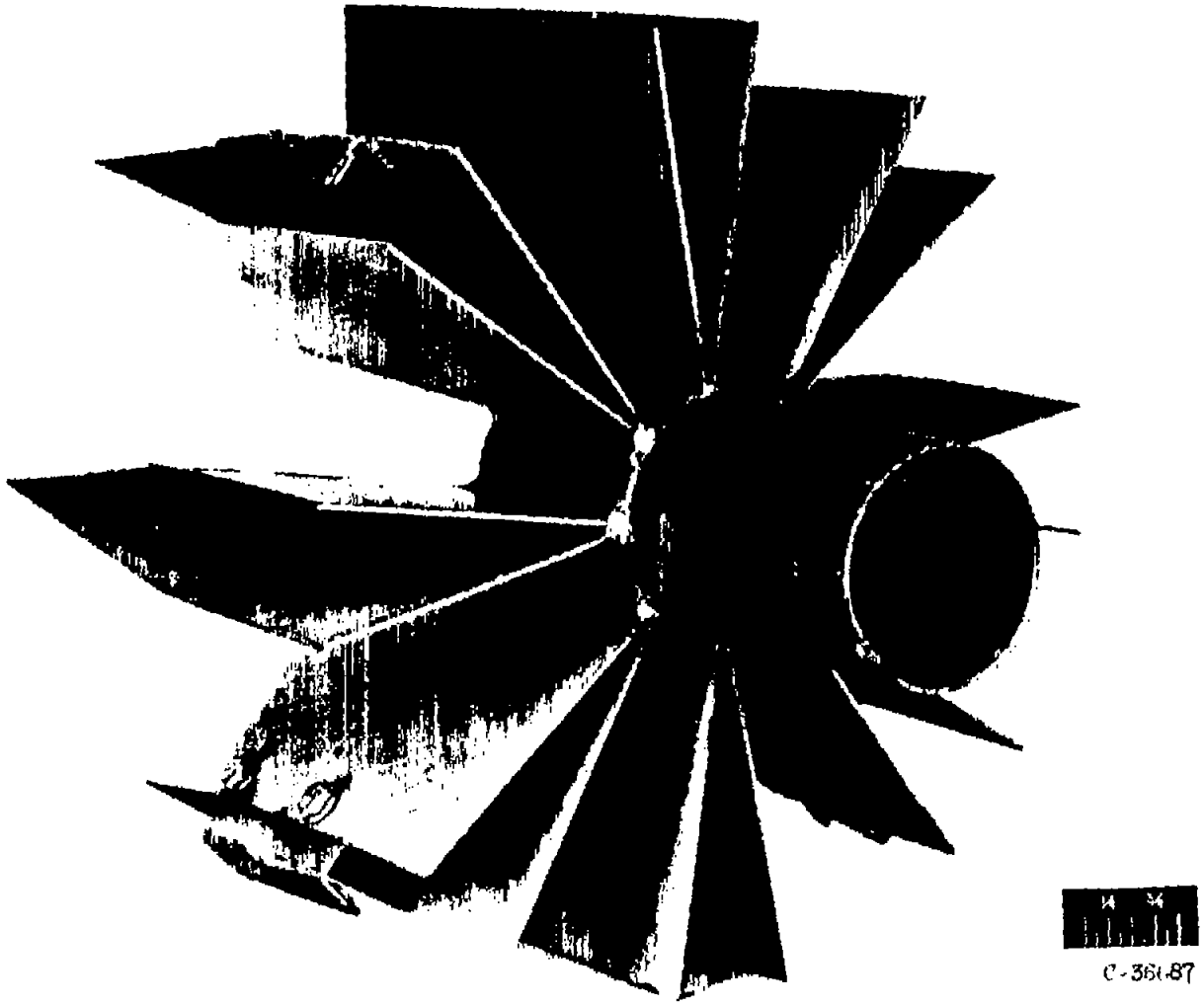

C-36687

Figure 3. - Flame holder and ignition flare holder.

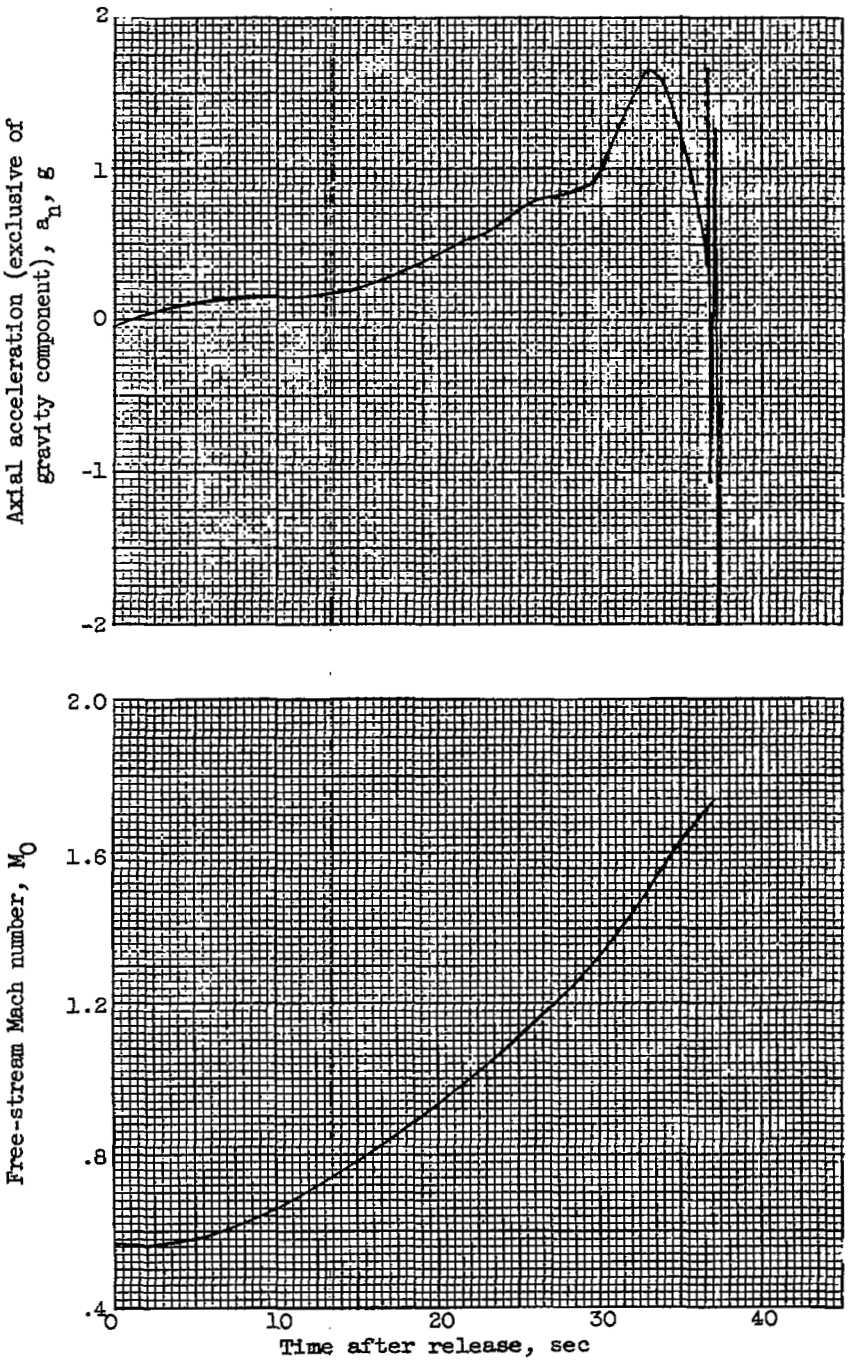

(a) Free-stream Mach number and axial acceleration.

Figure 4. - Time history of flight conditions.

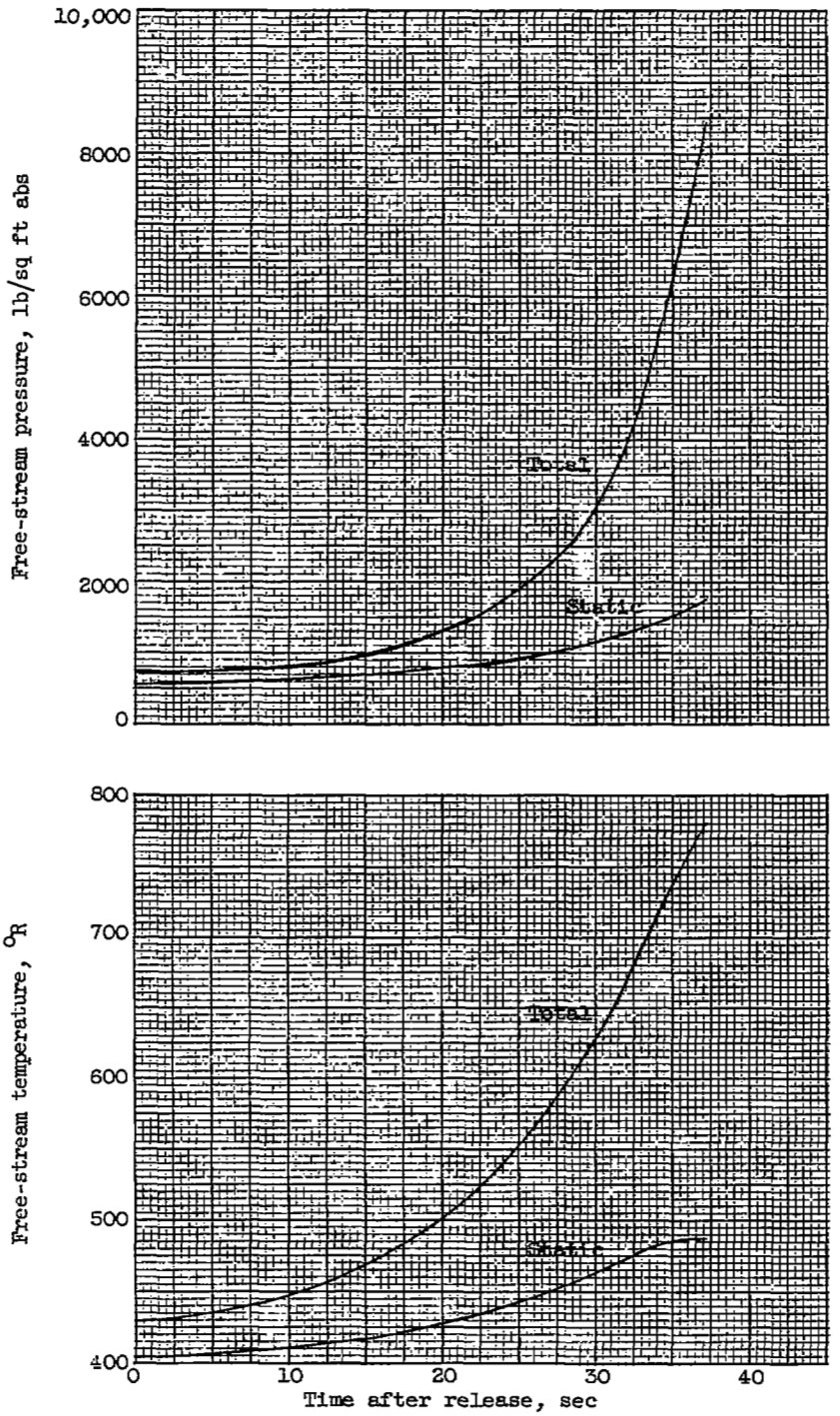

(b) Free-stream pressures and temperatures.

Figure 4. - Continued. Time history of flight conditions.

[redacted]

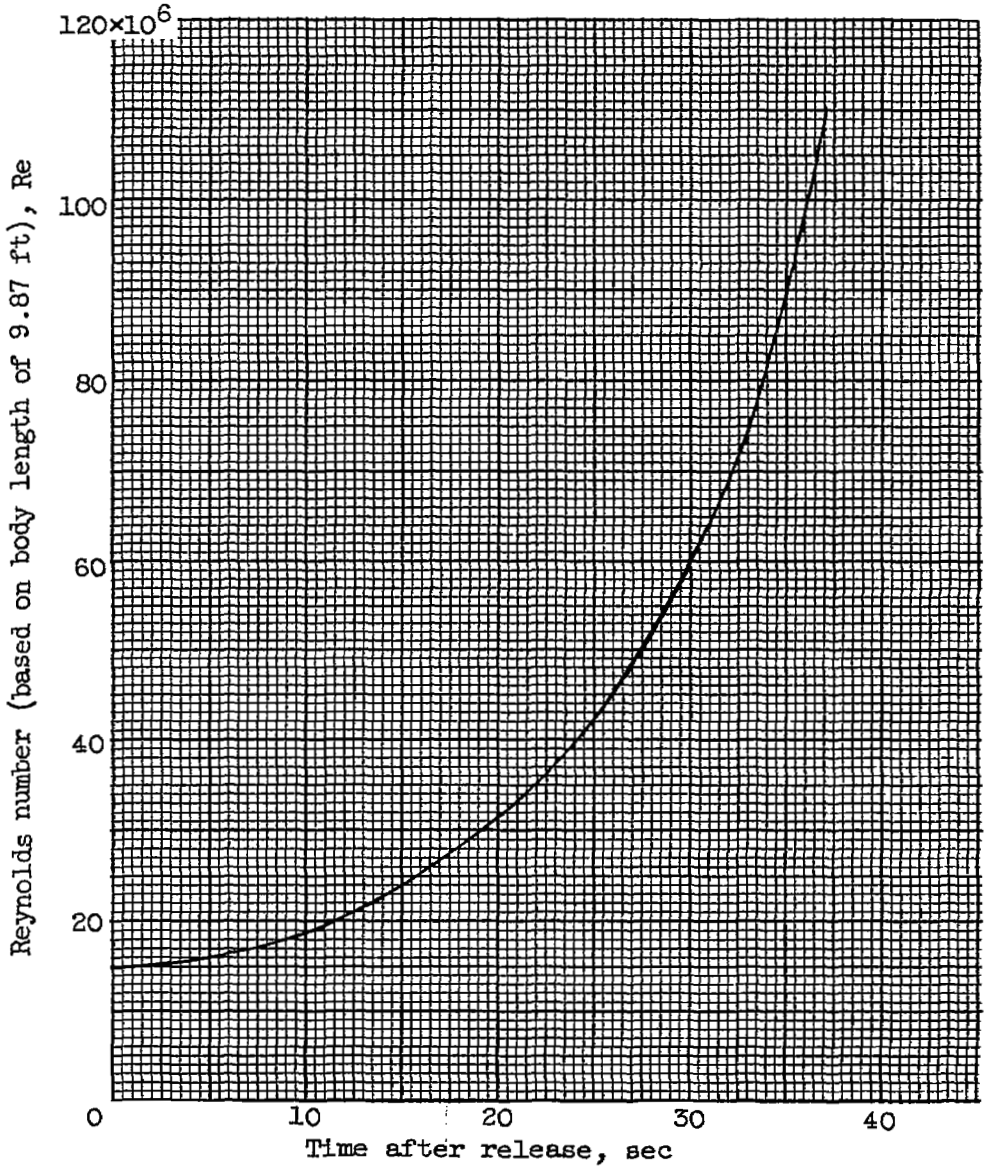

(c) Reynolds number.

Figure 4. - Concluded. Time history of flight conditions.

[redacted]

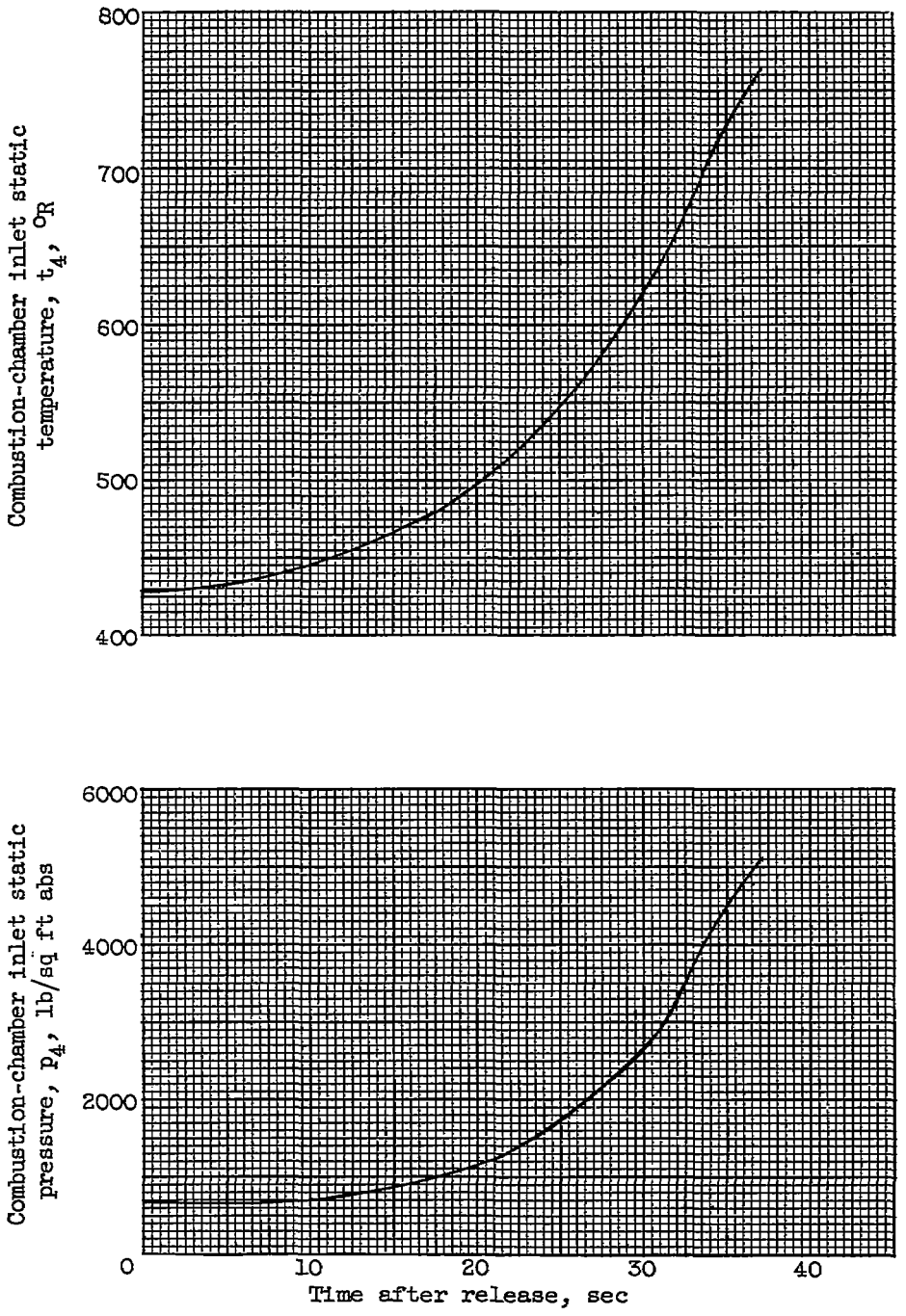

(a) Inlet static pressure and temperature.

Figure 5. - Time history of combustion-chamber conditions.

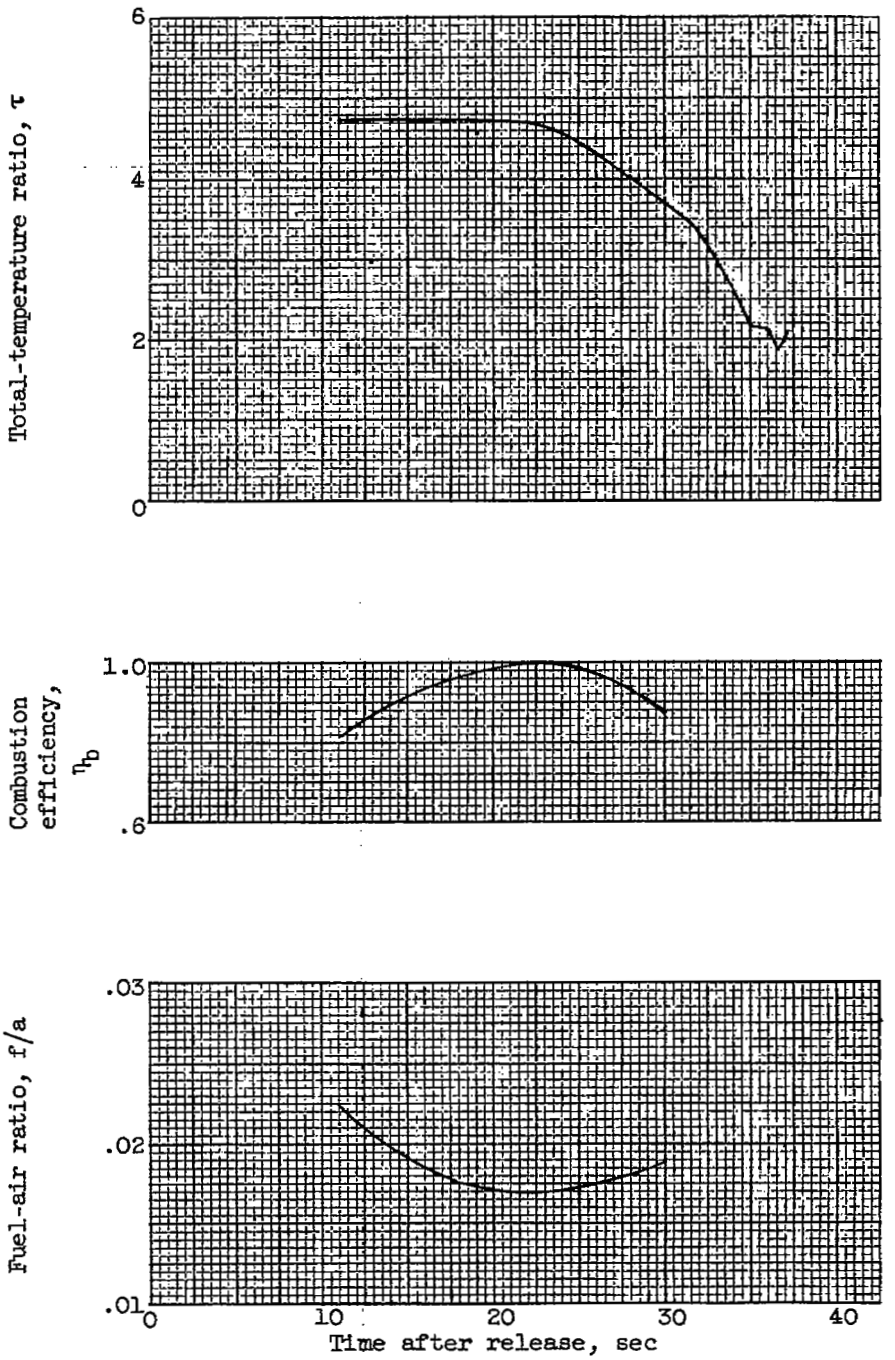

(b) Fuel-air ratio, combustion efficiency, and total-temperature ratio.

Figure 5. - Continued. Time history of combustion-chamber conditions.

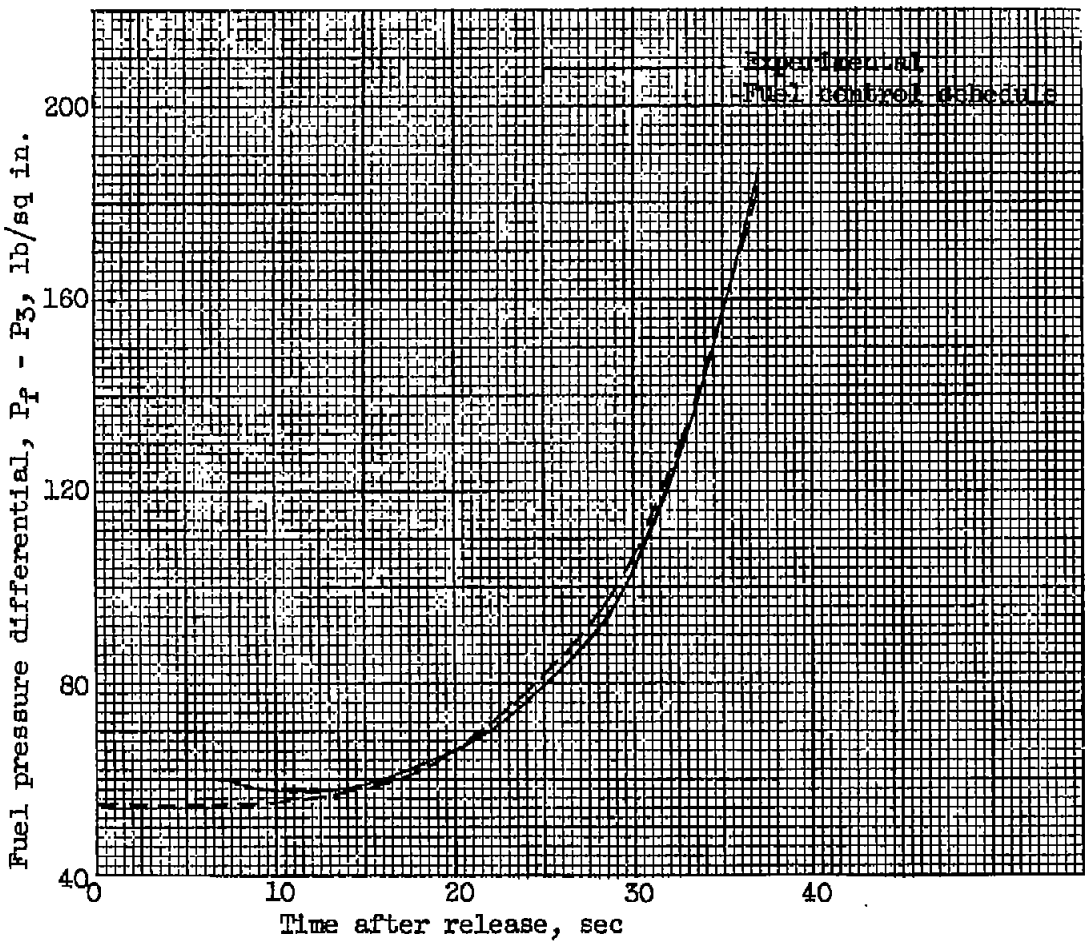

(c) Fuel pressure differential.

Figure 5. - Continued. Time history of combustion-chamber conditions.

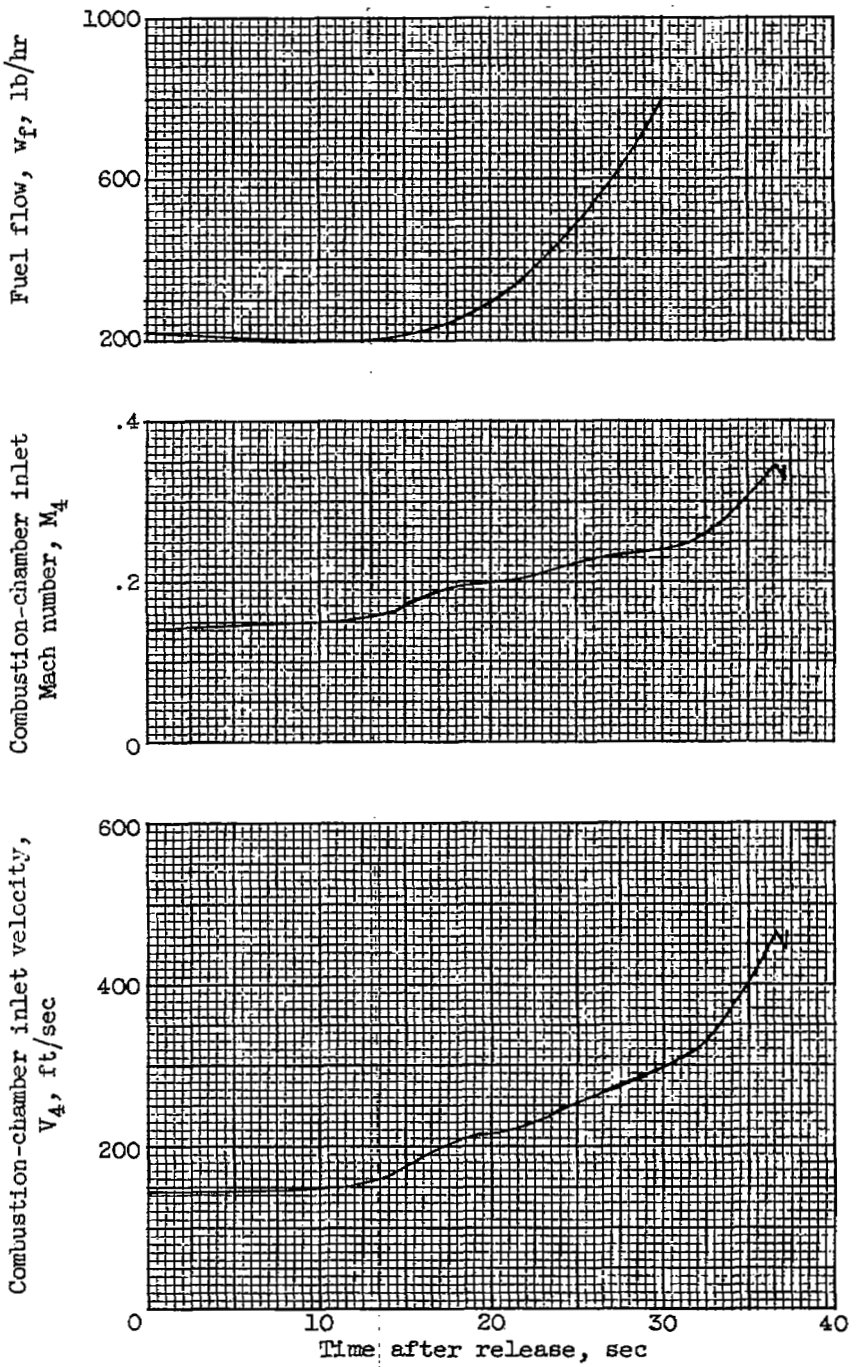

(d) Inlet velocity, inlet Mach number, and fuel flow.

Figure 5. - Concluded. Time history of combustion-chamber conditions.

[redacted]

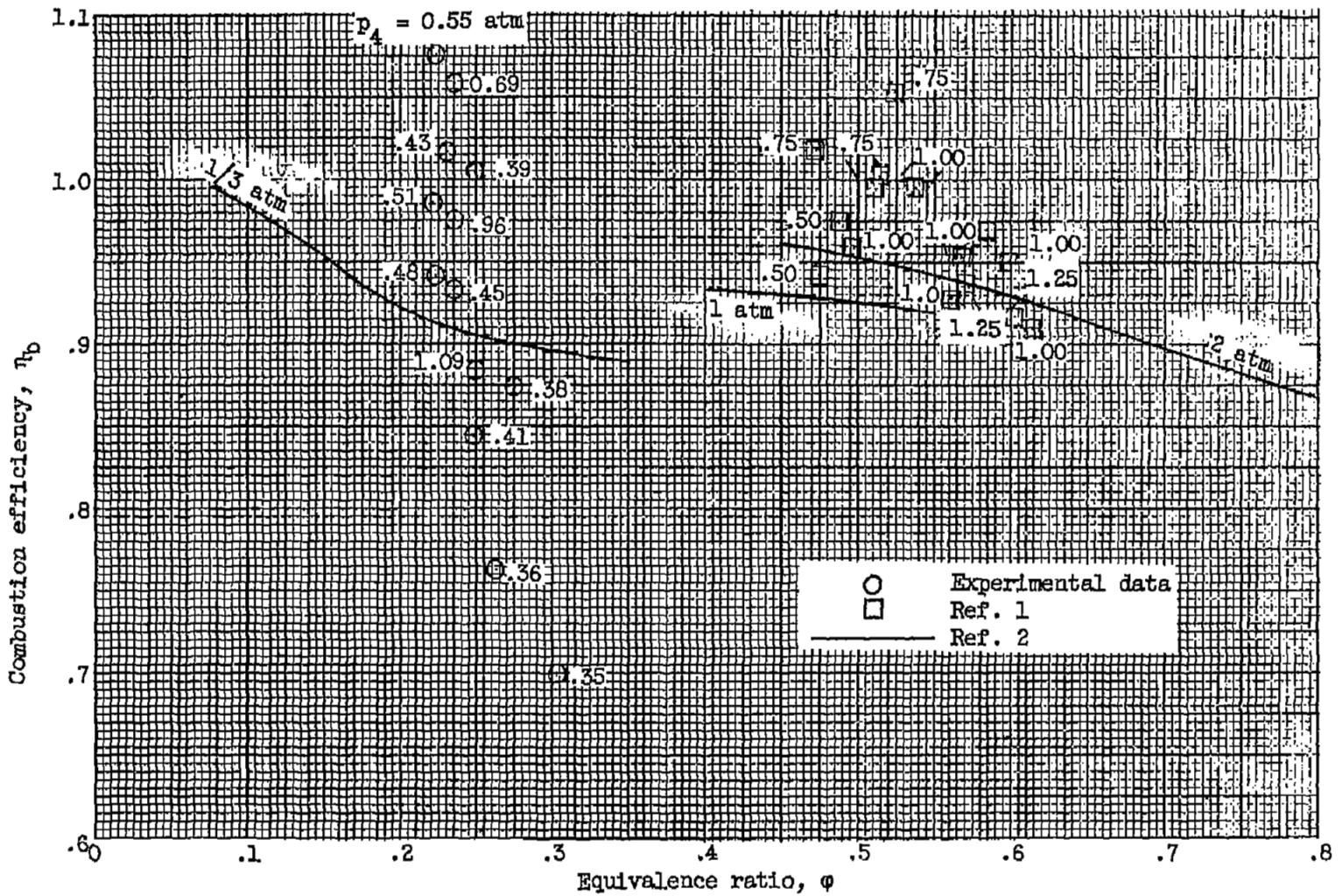

Figure 6. - Variation of combustion efficiency with equivalence ratio.

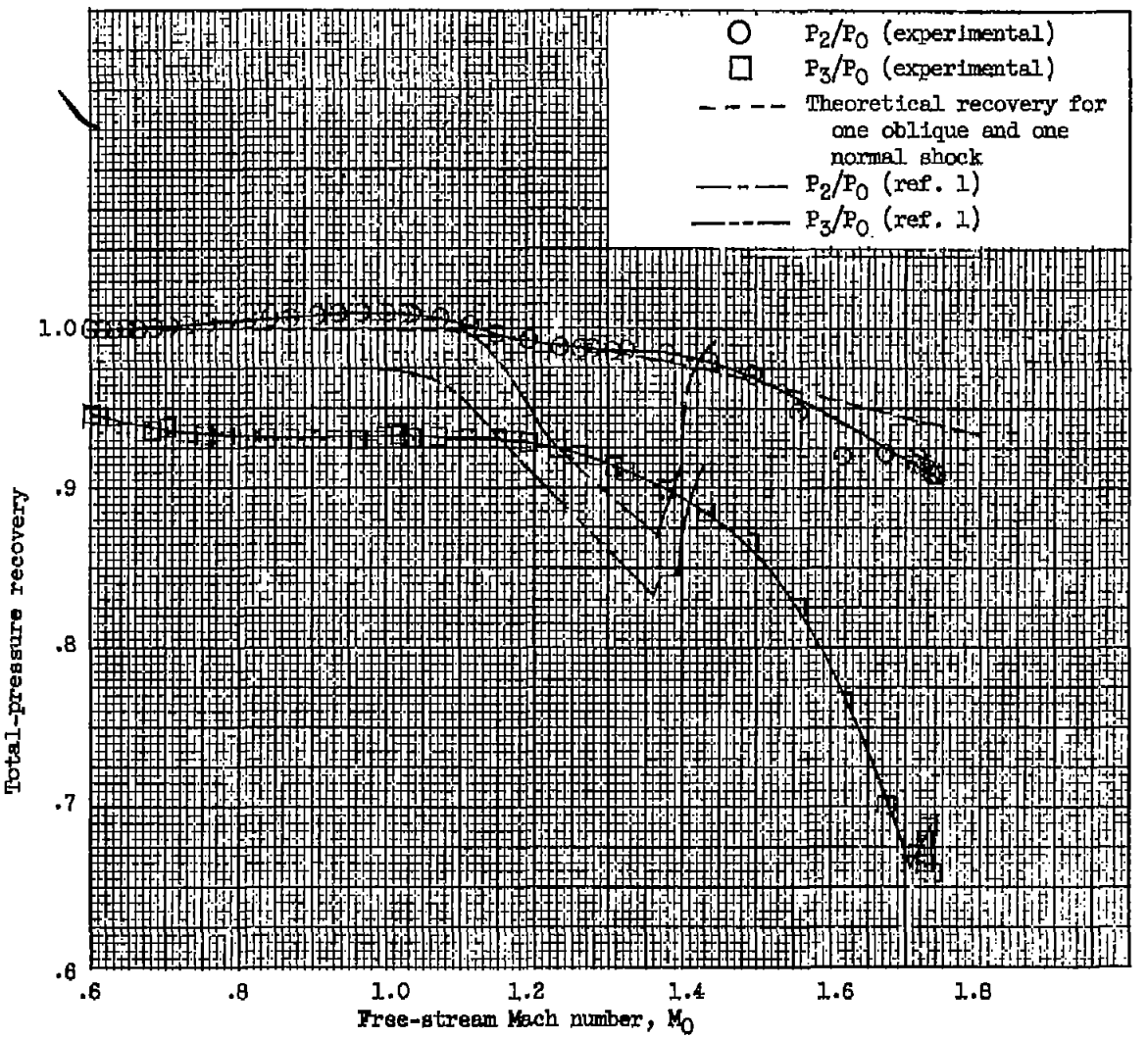

Figure 8. - Effect of free-stream Mach number on total-pressure recovery in the diffuser.

NACA – Digidocs

Document processing error

Unreadable tiff image

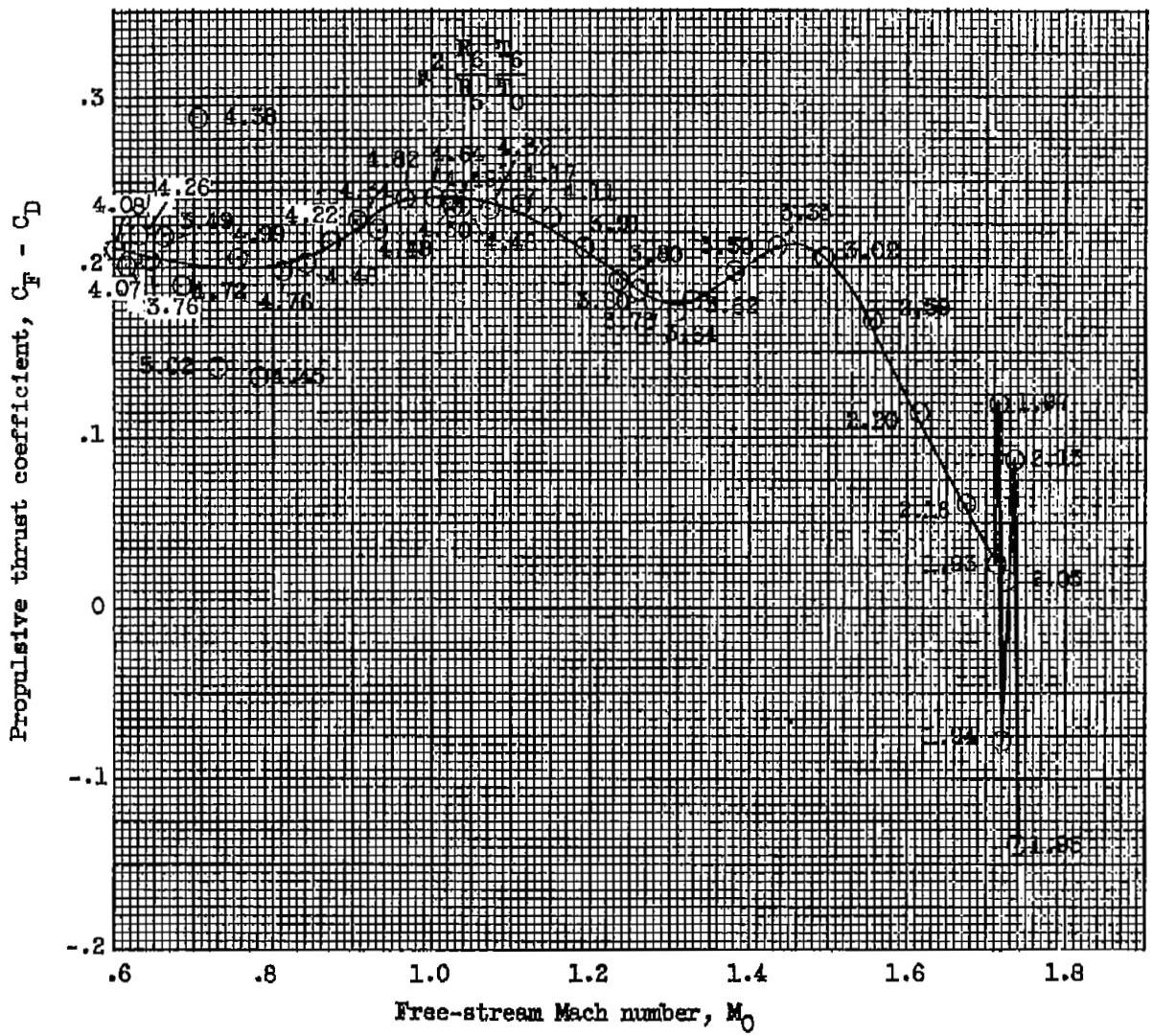

Figure 10 - Propulsive thrust coefficient as a function of free-stream Mach number.

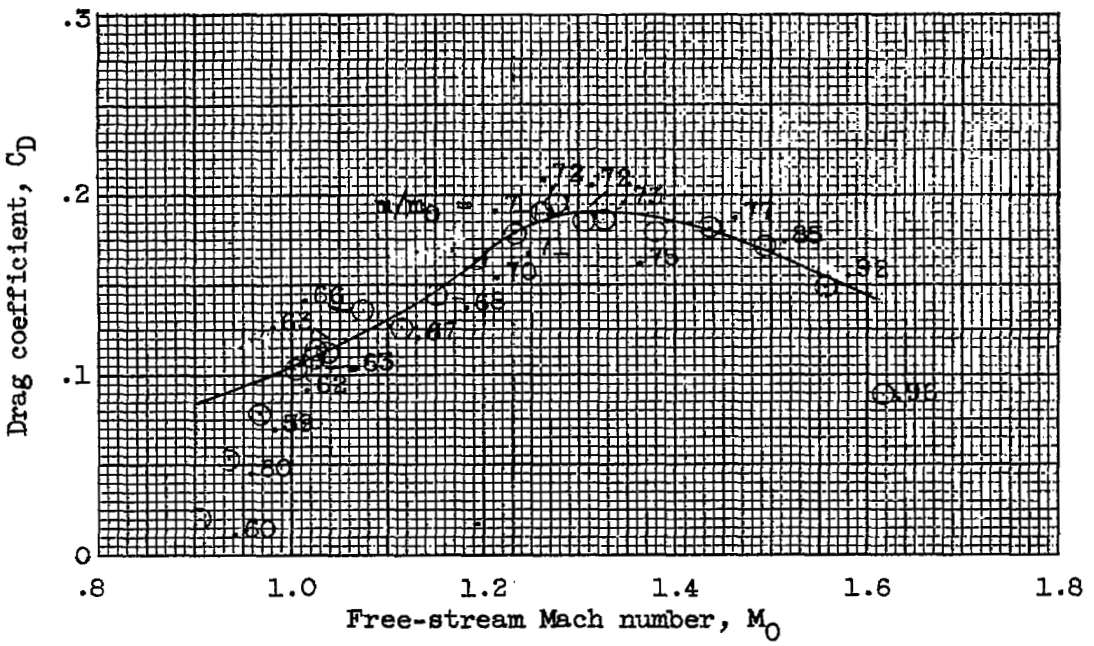

Figure 11. - Drag coefficient as a function of free-stream Mach number.

[redacted]

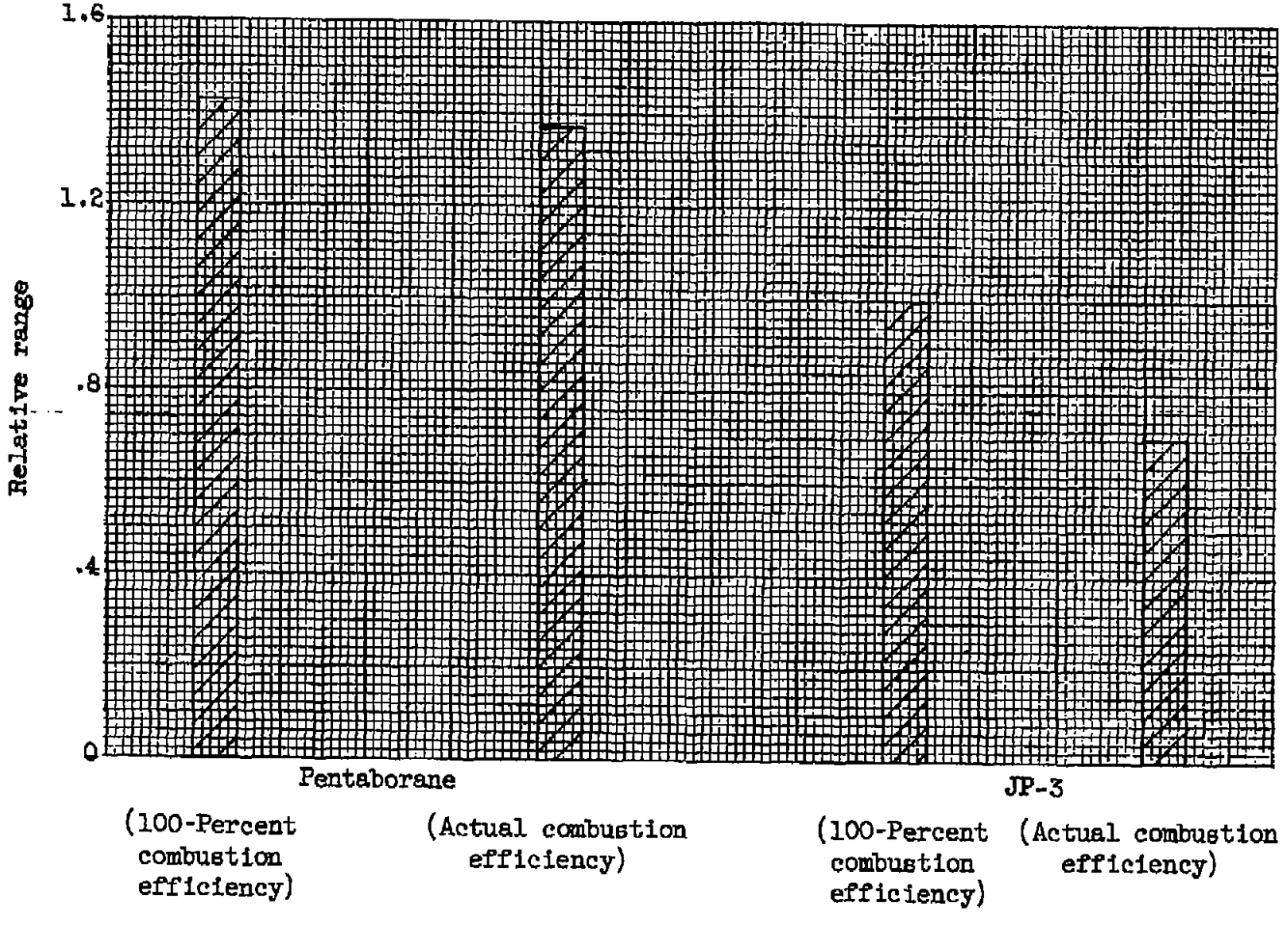

Figure 12. - Comparison of relative ranges of pentaborane and JP-3 fuels.